RSC Advances

This is an *Accepted Manuscript*, which has been through the Royal Society of Chemistry peer review process and has been accepted for publication.

Accepted Manuscripts are published online shortly after acceptance, before technical editing, formatting and proof reading. Using this free service, authors can make their results available to the community, in citable form, before we publish the edited article. This *Accepted Manuscript* will be replaced by the edited, formatted and paginated article as soon as this is available.

You can find more information about *Accepted Manuscripts* in the Information for Authors.

Please note that technical editing may introduce minor changes to the text and/or graphics, which may alter content. The journal's standard Terms & Conditions and the Ethical guidelines still apply. In no event shall the Royal Society of Chemistry be held responsible for any errors or omissions in this *Accepted Manuscript* or any consequences arising from the use of any information it contains.

ROYAL SOCIETY OF CHEMISTRY

www.rsc.org/advances

Please do not adjust margins

RSC Advances

ARTICLE

Formation of SiO_2@SnO_2 Core-Shell Nanofibers and Their Gas Sensing Properties

Received 00th January 20xx,
Accepted 00th January 20xx

DOI: 10.1039/x0xx00000x

www.rsc.org/

Yunshi Liu,[a] Ping Yang,*[a] Jia Li,[a] Katarzyna Matras-Postolek,[b] Yunlong Yue[a] Baibiao Huang[c]

SiO_2@SnO_2 core-shell nanofibers (NFs) were successfully prepared by single-spinneret electrospinning and subsquent calcination process. The precursor solutions were prepared from Poly(vinylpyrrolidone), SnO_2 precursors, and tetraethylorthosilicate (TEOS) with prehydrolysis. The pre-hydrolysis of TEOS plays an important role for the formation of core-shell structure. After calcining, the resulting fiber sample have an amorphous SiO_2 core and a shell consisted of SnO_2 particles. The fibers with various morphologies were obtained through adjusting the molar ratio of Sn and Si and the possible formation mechanism of core-shell NFs was proposed. Both Kirkendall effect and grain growth played important roles for the formation of core-shell structure. Furthermore, SiO_2 was used as support material to fix the SnO_2 particles and avoid the collapse of the SnO_2 structure. The amount of SnO_2 precursors directly determined the compactness of the shell, resulting in the different gas sensing properties. The SiO_2@SnO_2 core-shell NF network sensor responds to ethanol, ammonia, benzene, toluene, chloroform, and hexane gases, but it exhibited enhanced gas response to ethanol with a short response time. Those SnO_2 particles formed on the exterior of the fibers provided lots of contact area with the target gas to reduce resistance. In addition, the connectivity between particles also had certain influence on the electrical conductivity of the sample. The results demonstrate that single-spinneret electrospinning can also be used to prepare core-shell fibers with various applications.

Introduction

Significant progress has recently been achieved in developing oxide nanofibers (NFs) which have attracted considerable attention for their potential use in many applications such as energy conversion, catalysis, and chemical sensors.[1-3] In particular, many efforts have focused on the various synthetic methods of one dimensional (1D) nanostructures, including template-directed synthesis, self-assembly, phase separation, and electrospinning.[4-7] Among the above-mentioned methods, electrospinning is one of the most powerful methods for the preparation of NFs due to its advantages such as simplicity, cost effective, relatively high yield, and production with large length-diameter ratio.

More recently, core-shell NFs, as another type of a 1D nanostructure, have aroused a vast concern because of its different components in core and shell section. The incorporation of core-shell NFs into electronic devices exhibits great performance. There are two common approaches to fabricate core-shell NFs by electrospinning. One is the two-stage process, which started with ordinary electrospinning of the core section (stage 1) and was followed by the coating deposition of the shell section (stage 2).[8-10] The relevant steps of this method were complicated and it was hard to find ideal solution for coatings of the exterior as well. The other is a single-stage process, called coaxial electrospinning method, which equipped with a compound coannular nozzle.[11-13] According to the possible interactions between the two different precursor solutions, it was difficult to control the preparation process. In addition, the diameter of the products fabricated by this method was rather large due to the coaxial nozzle. On account of these complicated preparation processes, their commercialization and mass production are still problematic.

SnO_2, a wide bandgap (3.6 eV) n-type semiconductor, has been extensively used for gas sensing due to its high sensitivity and stability at operational temperature. When a SnO_2 sensor is placed in oxidizing ambient, the surface of SnO_2 absorbed oxygen molecules and then electrons are extracted from the surface leading to the increase of the depletion layer.[14-17] The electrospun NFs with a high surface-to-volume ratio for gas adsorption and desorption provide a potential application in gas sensors. The studies on the gas sensing properties of 1D SnO_2 nanostructures can be found in some literatures.[18-20] Kim et al fabricated SnO_2 nanotubes by combing electrospinning and atomic layer deposition and the gas sensing applications

[a] School of Material Science and Engineering, University of Jinan, Jinan, 250022, P.R. China, Fax: +86 531 87974453; Tel: +86 531 89736225; E-mail: mse_yangp@ujn.edu.cn
[b] Faculty of Chemical Engineering and Technology, Cracow University of Technology, Krakow, 31-155, Poland
[a,c] State Key Laboratory of Crystal Materials, Shandong University, Jinan, 250100, P. R. China

RSC Advances Accepted Manuscript

were also investigated.[18] Song and co-workers reported that ZnO/SnO_2 composite fibers were fabricated through a combination of surfactant-directed assembly and an electrospinning approach and the samples exhibited quick response and recovery in the range 3-500 ppm for ethanol.[19] For H_2 gas sensors, Kadir et al showed that aligned electrospun SnO_2 NFs operated at a low temperature of 150 °C.[20]

To the best our knowledge, there have been few researches focused on core-shell NFs prepared by a single-spinneret electrospinning method. In this paper, we successfully fabricated SiO_2@SnO_2 core-shell NFs by a single-spinneret electrospinning method using solutions with high-molecular polymer, SnO_2 precursors, and tetraethylorthosilicate (TEOS) with pre-hydrolysis and subsequent calcination process. The formation mechanism of 1D core-shell structure was proposed by systematical investigation. Fibers with various morphologies were obtained through adjusting the molar ratio of Sn and Si and their application in ethanol gas sensing was also studied.

Experimental

Materials

Ethanol, N,N-dimethylformamide (DMF), and ammonia was purchased from Tianjin Chemical Reagent Institute. Poly(vinylpyrrolidone) (PVP; M_w≈1,300,000) was taken from Aladdin Reagent Company. Tetraethylorthosilicate (TEOS) and $SnCl_2{\cdot}2H_2O$ were purchased from Sinopharm Chemical Reagent Company. All chemicals were analytical grade reagents and they were used directly without any further purification.

Preparation of SiO_2@SnO_2 core-shell NFs

Firstly, TEOS was mixed with ethanol and then $NH_3{\cdot}H_2O$ was added drop by drop with stirring. The mixed solution was allowed to stir for 3h, named as solution A. In addition, $SnCl_2{\cdot}2H_2O$ and PVP were dissolved in 6 mL of DMF with stirring for 12h, named as solution B. Solution A was added slowly into solution B to prepare a spinning solution. To confirm the morphological changes in composite NFs, the molar ratios of Sn and Si precursors was adjusted as 1:5, 1:4 1:3, and 1:1 to give sample names Sn-Si-5, Sn-Si-4, Sn-Si-3, and Sn-Si-1, respectively.

A typical electrospinning setup is made up of a high voltage DC power supply, a capillary and a grounded collector. Here, we use single-spinneret electrospinning to fabricate core-shell NFs. Each spinning solution was filled into a syringe with a volume of 5 mL and the syringe was equipped with a stainless steel needle with an inner diameter of 0.7 mm. A DC voltage of 15 kV was applied on the needle and a flat aluminum foil was placed 15cm below the needle to collect as-spun fibers. The optimal feed rate was 0.42 mL/h. After calcining the as-spun fibers at 550 °C for 3h with a heating rate at 5 °C min^{-1}, the final SiO_2@SnO_2 core-shell NFs were obtained. The preparation conditions were shown in Table 1.

Characterization

The morphology observation of samples was carried out using a field-emission scanning electron microscopy (FESEM, QUANTA 250 FEG, FEI, America). The transmission electron microscopy (TEM) images were recorded on a JEM-2010 transmission electron microscope and a transmission/scanning transmission electron microscope (TEM/STEM, Tecani F20, FEI). The particle size and the average diameter of samples were calculated based on randomly selected fibers. The crystal structures and phase composition of samples were observed using an X-Ray Diffraction (XRD) meter (Bruker D8-Advance, Germany).

Table 1. Preparation conditions and properties of samples.[a]

Sample	Sn/Si molar ratio	Average diameter (nm)	Response[b]	Response time (s)[b]	Recovery time (s)[b]
Sn-Si-5	1:5	160	9	21	29
Sn-Si-3	1:3	210	37	13	16
Sn-Si-1	1:1	320	14	16	17

[a]The size of SnO_2 NPs for Samples Sn-Si-5, Sn-Si-3, Sn-Si-1are 10, 50, and 80 nm, respectively. [b]The values are obtained at 200 ppm.

Gas sensing measurement

Gas sensing performance was obtained using a WS-30A system (Weisheng Instruments Co., Zhengzhou, China). The calcined sample was mixed with ethanol to form a paste. Then, the paste was coated uniformly on a ceramic tube, on which a pair of gold electrodes had been previously printed. A Cr-Ni heating wire was inserted into the ceramic tube as a resistor. Before measurement, the sensors were dried and aged for about 5 days. During the test process, the saturated target gas was injected into the test chamber (about 1 L) by a disposable syringe. After fully mixed with ambient air, the sensor was put into the chamber. The sensor was taken out to recover in ambient air after the response reached a constant value. The gas sensor resistance and response values were obtained by the analysis system automatically. When testing, a working voltage of 5 V was applied on the sensor. The response of the sensor in air or in a target gas could be measured by monitoring the voltage across the reference resistor. The gas sensor response value was defined as R_{air}/R_{gas}, where R_{air} is the electrical resistance of the sensor in air and R_{gas} is the resistance of sensor in the presence of the target gas. The response time in the case of adsorption or the recovery time in the case of desorption was defined as the time taken by the sensor to achieve 90 % of the total resistance change.

Results and discussion

The morphology of as-spun fibers was determined by SEM observation as shown in Figure 1a. Before heat treatment, the as-spun fibers exhibited uniform and well-dispersed NF morphology with an average diameter of ~410 nm. From the image with low magnification, the fibers were randomly

RSC Advances Accepted Manuscript

This journal is © The Royal Society of Chemistry 20xx

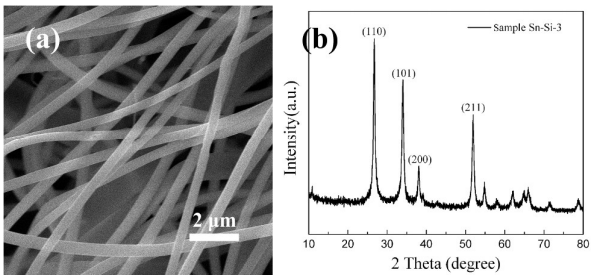

Figure 1. (a) SEM image of as-spun fibers; (b) XRD patterns of sample Sn-Si-3.

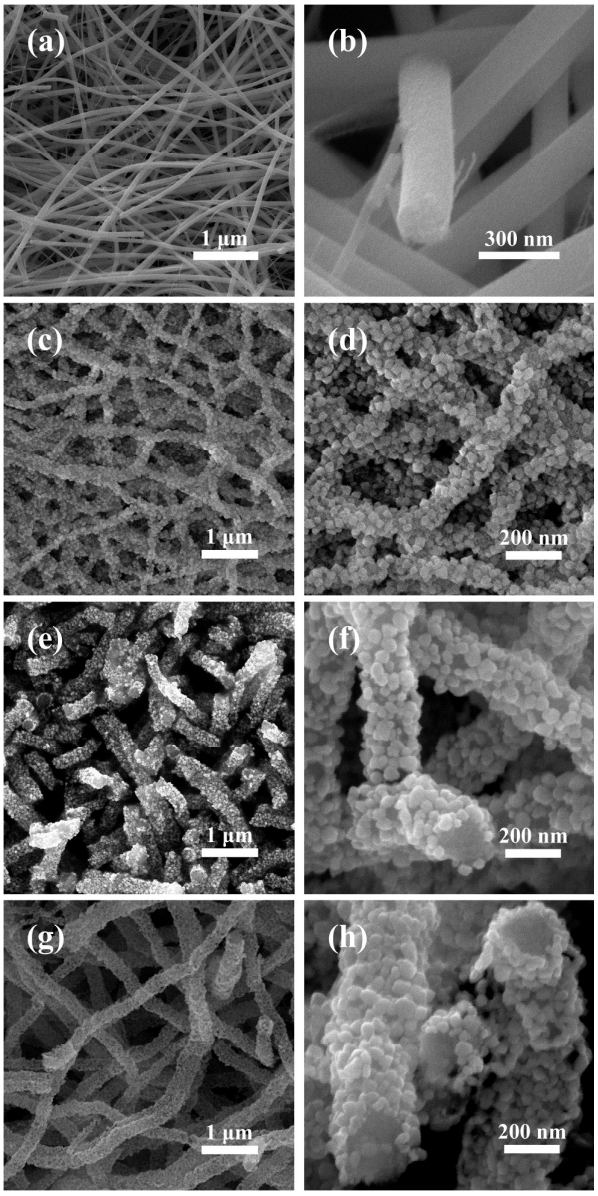

Figure 2. SEM images of (a, b) sample Sn-Si-5; (c, d) sample Sn-Si-4; (e, f) sample Sn-Si-3; (g, h) sample Sn-Si-1.

arranged due to the unstable bending process during electrospinning. XRD measurements were purposely carried out to provide further insight into the crystallinity of the samples. Figure 1b shows the XRD patterns of sample Sn-Si-3 heat-treated with calcination at 550 °C. No diffraction peaks corresponding to impurities are observed, indicating the high purity of the products. Characteristic diffraction peaks at 26.6°, 33.9°, 38.1° and 51.8° are obtained, corresponding to a SnO_2 phase with tetragonal structure (JCPDS card No. 41-1445). Furthermore, no characteristic peaks relative to SiO_2 are obtained, suggesting the amorphous phase of SiO_2. The XRD analysis results indicated that the composite fibers were composed of two components including well-crystallized SnO_2 and amorphous SiO_2.

Figure 2 shows the SEM images of samples Sn-Si-5, Sn-Si-4, Sn-Si-3, and Sn-Si-1 after they were calcined at 550 °C. As listed in table 1, the diameters of the SiO_2@SnO_2 core-shell NFs were in the range of ~160 nm for sample Sn-Si-5, ~210 nm for sample Sn-Si-3, and ~320 nm for sample Sn-Si-1. As shown in figure 2a and b, few small particles were embedded on the exterior of the fibers, indicating a relative smooth surface on the composite fibers. Figure 2c to h showed that as the amount of SnO_2 increased, samples exhibited rough surface on the fibers, suggesting lots of SnO_2 or SiO_2 particles formed on the fibers. From the cross section of the fibers, the image with different contrast shows the interesting distribution of the two components. As the contents of SnO_2 increased, the core-shell structure became more apparent. The particles were uniformly distributed on the fiber surface, which may provide more contact area during their applications. In addition, the porous properties of the SiO_2/SnO_2 core-shell nanofibers were very similar with pure SiO_2 fibers prepared via a similar method with the core-shell one although a SnO_2 particle shell coated.

In order to further investigate the structural and morphology properties of the NFs, TEM examinations were carried out. The inset in Figure 3a shows the electronic diffraction spectroscopy (EDS) spectrum of sample Sn-Si-3, indicating the composition of both SnO_2 and SiO_2. This was consistent with the results from XRD patterns. The fibers had large length-diameter ratio, as shown in Figure 3b. The TEM images shown in Figure 3c and d clearly confirm the core-shell structure and the distribution of the two components. The inner section was composed of amorphous SiO_2 to form core fiber and the outer section was made up of uniform SnO_2 particles to form shell of the fiber. The crystal structures can be observed by high-magnification TEM, as shown in Figure 3d and e. The lattice fringes with a spacing of 0.334 nm can be observed, which is in agreement with the spacing of (110) planes of SnO_2. Furthermore, the clear crystal lattice shows the good crystallinity of sample Sn-Si-3. The results suggested that the samples had obvious core-shell structure with interesting distributions of components, indicating that single-spinneret electrospinning method could be used to fabricate core-shell NFs as well.

On the basis of experimental observations, a possible formation mechanism of SiO_2@SnO_2 core-shell NFs was proposed. During the preparation of spinning solution, the SiO_2

RSC Advances Accepted Manuscript

monomers formed in the course of TEOS hydrolysis in an ethanol-water-ammonia medium condensed to give primary SiO_2 particles.[21] After electrospinning, the composite as-spun fibers were obtained on the collector. The composite fiber was made up of $SnCl_2$, SiO_2, PVP, and solvents. In addition, all the materials were randomly distributed in the fiber and the composite fiber, as shown in step (b) in Scheme 1. As the temperature increased, the solvents, including ethanol and DMF, evaporated from fiber to the ambient. It was worth mentioning that the effect of evaporation of solvent on the movement of metal ions was very important. Due to the higher solubility in ethanol and DMF than in PVP, Sn ions were carried to the surface layer of the fiber.[22] In contrast, SiO_2 composites were retained to form Si-rich part in the center of the fibers. When the calcining temperature was high enough, Sn ions crystallized to form SnO_2 and PVP decomposed to NO_2, CO_2, and H_2O. Sn ions of the outer section oxidized more rapidly than that of the inner section as the surface of fiber was exposed to reactant oxygen in air. Thus, a concentration gradient existed in the fiber and the SnO_2 shell formed on the surface of the fiber. During this process, Kirkendall effect played a significant role in the Sn ions movement. At the same time, SiO_2 particles aggregated to form the core fiber due to the solvent evaporation and the rising temperature. In addition, with further increasing temperature, inorganic salts were completely transformed into metal oxide particles, forming the shell of the fibers. After calcining for 3h, SiO_2@SnO_2 core-shell NFs were obtained. In general, both Kirkendall effect and grain growth played important roles in the formation of core-shell structure. Core-shell nanostructures could be prepared by adjusting the precursor ratio and composition of the spinning solutions via single-spinneret electrospinning method.

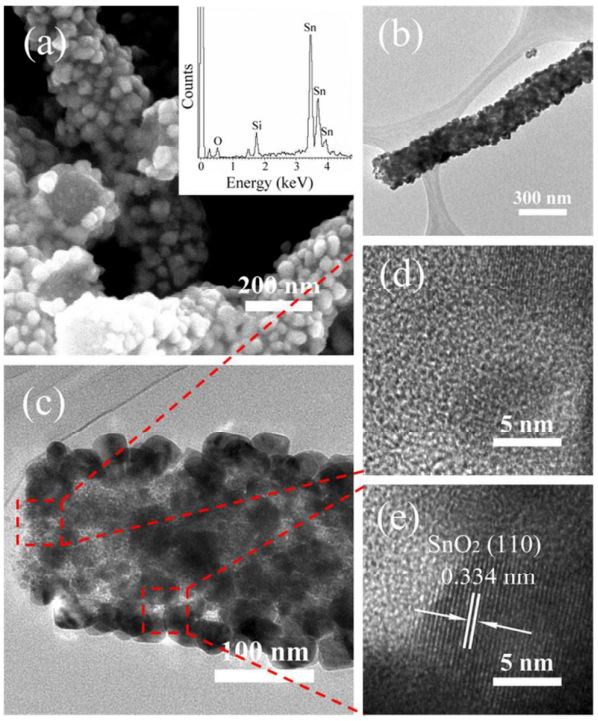

Figure 3. (a) SEM image, (b, c) TEM images, and (d, e) HRTEM images of sample Sn-Si-3. Inset in (a) shows the EDS spectrum of sample Sn-Si-3.

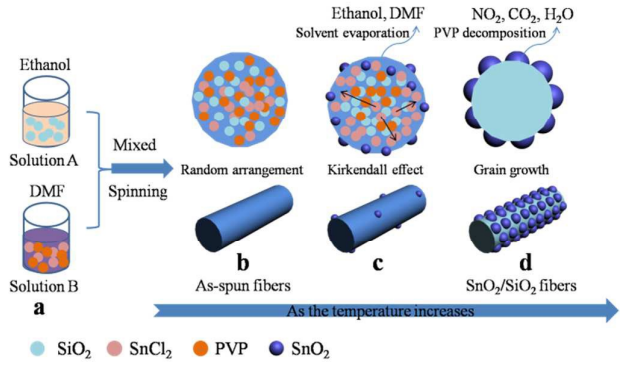

Scheme 1. Schematic of (a) spinning solution, (b) as-spun fibers, (c) fibers during calcinations, and (d) composite SnO_2@SiO_2 fibers.

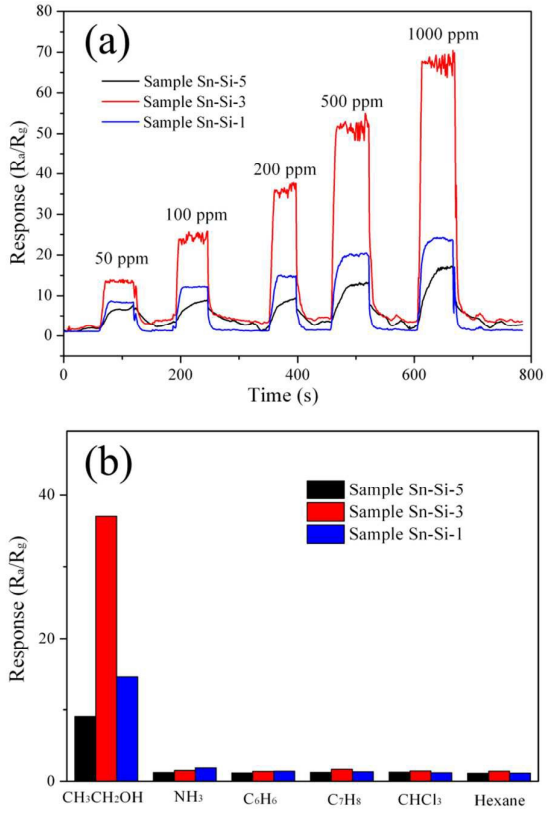

Figure 4. (a) Response and recovery characteristic curves of SnO_2@SiO_2 nanostructures based sensor to 50-1000 ppm ethanol, respectively; (b) the cross-response of the sensors to 200 ppm ethanol, ammonia, benzene, toluene, chloroform, and hexane.

RSC Advances Accepted Manuscript

This journal is © The Royal Society of Chemistry 20xx

It is important to investigate the influence of different morphologies and special core-shell structure on their application performance. As shown in Figure 4a, the responses of SiO_2@SnO_2 core-shell NFs towards ethanol sensing properties were measured at different concertrations, ranging from 50 to 1000 ppm. In an air ambience, oxygen molecules adsorb on the surface of the core-shell NFs and form oxygen ions (O^-, O^{2-}).[23] This process would capture electrons from the conduction band, resulting in a high resistance state of the samples. When the core-shell NFs were exposed to ethanol, the absorbed oxygen ions react with the reducing gas. In this case, the samples released electrons to the conduction band and resulted in the decrease of resistance. After the target gas was removed, the resistance of the samples returned to the original value due to the desorption of oxygen.

Sample Sn-Si-3 exihibited higher gas sensing performance with a response of ~37 at 200 ppm than that of smples Sn-Si-5 and Sn-Si-1. The response and recovery time of different samples were observed and compared as well. It can be observed that in smples Sn-Si-5, Sn-Si-3 and Sn-Si-1, the response tiime to 200 ppm ethanol were determined to be ~21, 13, and 16s, while the recovery time of them to be ~29, 16, and 17s, respectively. The details were shown in table 1. Therefore, it can be concluded that the ratio of Sn and Si played important role in gas sensing performance of the composites. Sample Sn-Si-5 had the smaller response among the samples due to the less amount of SnO_2 in the shell section. When the amount of SnO_2 was too much, the surface of the fiber was fully composed of SnO_2, resulting in the less contact area with ethanol.

The selective test towards ethanol, ammonia, benzene, toluene, chloroform, and hexane were determined. As shown in Figure 4b, all the samples exhibited better selectivity to ethanol, indicating their potential application in complicated circumstance. When the ratio of Sn and Si was 1:3, the sensor showed excellent sesentivity to 200 ppm ethanol while has very small response to the other typical gases at the same temperature.

As listed in Table 1, the particle size of the SnO_2 shell were in the range of ~10 nm for sample Sn-Si-5, ~50 nm for sample Sn-Si-3, and ~80 nm for sample Sn-Si-1. Some previous reports suggested that the sensor response to gases is proportional to the reciprocal of particle size.[24,25] Therefore, the response to ethanol of sample Sn-Si-3 was higher than that of sample Sn-Si-5. However, sample Sn-Si-5 which had the smallest size among these samples exhibited the worst gas sensing performance. This phenomenon may be due to the low amount of SnO_2 on the fibers. It should be mentioned that the special core-shell structure also had an important effect on the gas sensing properties except for ratio of Sn and Si. The 1D core-shell structure can significantly increase the surface-to-volume ratio, which may provide more contact area with the target gases. Furthermore, SiO_2 core section could enhance the structural stability. And comparing to powder samples, it could also fix the SnO_2 particles on the surface of the fiber to decrease the aggregation degree of the particles. In addtion, the 1D structure could also accelerate the electron tansfer rate during gas sensing test. All the samples did not have highest response and recovery time comparing to the other SnO_2 materials. This could be because of the connection between the SnO_2 particles in the shell section of the fiber.

Conclusions

SiO_2@SnO_2 core-shell NFs were prepared by a single-spinneret electrospinning route and subsequent calcination process. Various morphological fibers were obtained through adjusting the molar ratio of Sn and Si. The inner section was composed of amorphous SiO_2 to form fiber core and the outer layer was consisted of uniform SnO_2 particles to form the shell of the fiber. The possible formation mechanism of the core-shell 1D structure was proposed. Sample Sn-Si-3 exhibited better response to 200 ppm ethanol and rapid response and recovery time during the test. Furthermore, The gas sensing properties of these samples to ethanol were investigated. Both the ratio of Sn and Si and the special core-shell structure played significant roles in gas sensing performance. It is found that core-shell 1D nanostructures could be prepared by adjusting the precursor ratio and composition of the spinning solutions via single-spinneret electrospinning method.

Acknowledgements

This work was supported in part by the project from National Basic Research Program of China (973 Program, 2013CB632401), the program for Taishan Scholars, the projects from National Natural Science Foundation of China (grant no. 51572109, 51501071, 51302106, 51402123, and 51402124).

1 Q. Zhang, E. Uchaker, S. L. Candelaria and G. Cao, *Chem. Soc. Rev.*, 2013, **42**, 3127.
2 W. H. Ryu, T. H. Yoon, S. H. Song, S. Jeon, Y. J. Park and I. D. Kim, *Nano lett.*, 2013, **13**, 4190.
3 A. Katoch, G. J. Sun, S. W. Choi, J. H. Byun and S. S. Kim, *Sensor. Actuat. B-Chem.*, 2013, **185**, 411.
4 H. Acar, R. Garifullin and M. O. Guler, *Langmuir*, 2011, **27**, 1079.
5 S. Y. Zhang, M. D. Regulacio and M. Y. Han, *Chem. Soc. Rev.*, 2014, **43**, 2301.
6 K. Sun and C. J. Bolech, *Phys. Rev. A*, 2013, **87**, 053622.
7 Y. Liu, H. S. Chen, J. Li and P. Yang, *RSC Adv.*, 2015, **5**, 37585.
8 M. Bognitzki, H. Hou, M. Ishaque, T. Frese, M. Hellwig, C. Schwarte, A. Schaper, J. H. Wendorff and A. Greiner, *Adv. Mater.*, 2000, **12**, 637.
9 M. Bognitzki, W. Czado, T. Frese, A. Schaper, M. Hellwig, M. Steinhart, A. Greiner and J. H. Wendorff, *Adv. Mater.*, 2001, **13**, 70.
10 W. Liu, M. Graham, E. A. Evans and D. H. Reneker, *J. Mater. Res.*, 2002, **17**, 3206.
11 Z. Sun, E. Zussman, A. L. Yarin, J. H. Wendorff and A. Greiner, *Adv. Mater.*, 2003, **15**, 1929.
12 I. G. Loscertales, A. Barrero, M. Márquez, R. Spretz, R. Velarde-Ortiz and G. Larsen, *J. Am. Chem. Soc.*, 2004, **126**, 5376.
13 J. H. Yu, S. V. Fridrikh and G. C. Rutledge, *Adv. Mater.*, 2004, **16**, 1562.

RSC Advances Accepted Manuscript

14 C. S. Moon, H. R. Kim, G. Auchterlonie, J. Drennan and J. H. Lee, *Sensor. Actuat. B-Chem.*, 2008, **131**, 556.
15 Y. Zhang, X. He, J. Li, Z. Miao and F. Huang, *Sensor. Actuat. B-Chem.*, 2008, **132**, 67.
16 G. X. Wang, J. S. Park, M. S. Park and X. L. Gou, *Sensor. Actuat. B-Chem.*, 2008, **131**, 313.
17 J. Huang, N. Matsunaga, K. Shimanoe, N. Yamazoe and T. Kunitake, *Chem. Mater.*, 2005, **17**, 3513.
18 W. S. Kim, B. S. Lee, D. H. Kim, H. C. Kim, W. R. Yu and S. H. Hong, *Nanotechnology*, 2010, **21**, 245605.
19 X. Song, Z. Wang, Y. Liu, C. Wang and L. Li, *Nanotechnology*, 2009, **20**, 075501.
20 R. A. Kadir, Z. Li, A. Z. Sadek, R. A. Rani, A. S. Zoolfakar, M. R. Field, J. Z. Ou, A. F. Chrimes and K. Kalantar-zadeh, *J. Phys. Chem. C*, 2014, **118**, 3129.
21 E. Y. Trofimova, D. A. Kurdyukov, S. A. Yakovlev, D. A. Kirilenko, Y. A. Kukushkina, A. V. Nashchekin, A. A. Sitnikova, M. A. Yagovkina and V. G. Golubev, *Nanotechnology*, 2013, **24**, 155601.
22 B. Lu, C. Zhu, Z. Zhang, W. Lan and E. Xie, *J. Mater. Chem.*, 2012, **22**, 1375.
23 Y. J. Chen, X. Y. Xue, Y. G. Wang and T. H. Wang, *Appl. Phys. Lett.*, 2005, **87**, 233503.
24 T. Kida, S. Fujiyama, K. Suematsu, M. Yuasa and K. Shimanoe, *J. Phys. Chem. C*, 2013, **117**, 17574.
25 X. Wan, J. Wang, L. Zhu and J. Tang, *J. Mater. Chem. A*, 2014, **2**, 13641.

RSC Advances Accepted Manuscript

 This journal is © The Royal Society of Chemistry 20xx

Graphical Abstract

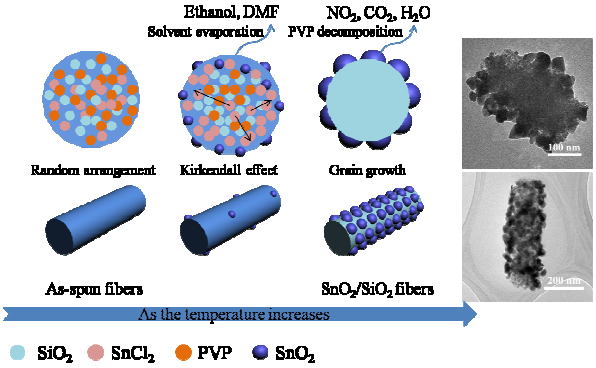

SiO_2@SnO_2 core-shell nanofibers were prepared by a single-spinneret electrospinning rote and subsequent calcination process. Both the ratio of Sn and Si and the special core-shell structure played significant roles in gas sensing performance.

RSC Advances Accepted Manuscript